

# Structure and Reactivity of Homocysteine Radical Cation in the Gas Phase Studied by Ion–Molecule Reactions and Infrared Multiple Photon Dissociation

Sandra Osburn,<sup>†</sup> Ticia Burgie,<sup>†</sup> Giel Berden,<sup>‡</sup> Jos Oomens,<sup>‡,§</sup> Richard A. J. O'Hair,<sup>||,⊥,#</sup> and Victor Ryzhov<sup>\*,†</sup>

<sup>†</sup>Department of Chemistry and Biochemistry, and Center for Biochemical and Biophysical Studies, Northern Illinois University, Dekalb, Illinois 60115, United States

<sup>‡</sup>FOM Institute for Plasma Physics Rijnhuizen, Nieuwegein, The Netherlands

<sup>§</sup>University of Amsterdam, Amsterdam, The Netherlands

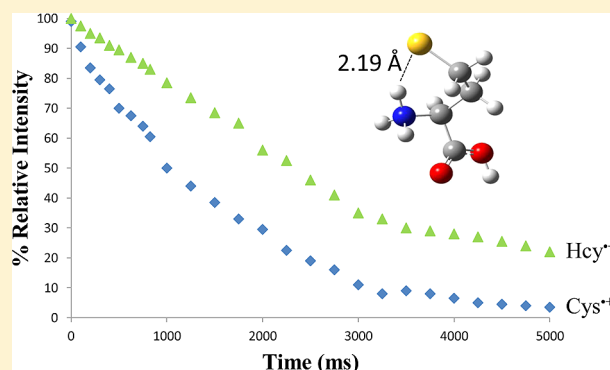
<sup>||</sup>School of Chemistry, The University of Melbourne, Melbourne, Victoria 3010, Australia

<sup>⊥</sup>Bio21 Institute of Molecular Science and Biotechnology, The University of Melbourne, Melbourne, Victoria 3010, Australia

<sup>#</sup>ARC Centre of Excellence for Free Radical Chemistry and Biotechnology, Melbourne, Victoria 3010, Australia

## S Supporting Information

**ABSTRACT:** The reactivity of the cysteine (Cys) and homocysteine (Hcy) radical cation was studied using ion–molecule reactions. The radical cations were generated via collision-induced dissociation (CID) of their S-nitrosylated precursors. Cleavage of the S–NO bond led to the formation of the radical initially positioned on the sulfur atom. The reactions of the radical cations with dimethyl disulfide revealed that the cysteine radical cation reacts more quickly than the homocysteine radical cation. Infrared multiple photon dissociation (IRMPD) spectroscopy and density functional theory (DFT) calculations were used to determine the structure of the homocysteine radical cation, which was compared to the previously published structure of the cysteine radical cation (Sinha et al. *Phys. Chem. Chem. Phys.* **2010**, *12*, 9794–9800). IRMPD spectroscopy and DFT calculations revealed that this difference in radical reactivity was not a result of a radical rearrangement for the homocysteine radical cation but rather that the reactivity was modulated by stronger hydrogen bonding.



## INTRODUCTION

Radicals are known to play critical roles in the active sites of some enzymes, often acting as reactive intermediates.<sup>1–12</sup> The radical site is usually generated on the side chain of certain amino acids, such as (1) tyrosine in class I ribonucleotide reductases,<sup>3</sup> (2) tryptophan in cytochrome oxidases,<sup>12</sup> (3) glycine in class III ribonucleotide reductases,<sup>8</sup> and (4) cysteine in pyruvate formate lyases.<sup>2</sup> Radical migration has been known to occur in some of these enzymes when they are in their inactive state.<sup>5,6,11</sup> This radical migration is believed to function so that the radical is not involved in unwanted side reactions but rather retained, thereby avoiding the energetically costly regeneration of the radical.<sup>5</sup> While radicals are useful in these enzymes when they are under strict control, if they are generated at the wrong place or at the wrong time, they can become very destructive.<sup>13–19</sup> This uncontrolled state can often lead to oxidation of side chains, fragmentation, cross-linking, and possibly changes in conformation.<sup>13–19</sup> All of these

reactions can potentially lead to the loss of function in a protein.

Over the years, mass spectrometry has become a very important tool in studying small model systems containing radical ions. This is largely due to the advances which have allowed for the easy generation and manipulation of these ions in the gas phase.<sup>20–31</sup> These methods often involve the chemical modification of an amino acid or peptide followed by collision-induced dissociation (CID). Siu and co-workers first introduced this concept by generating radical cations of amino acids through CID of metal complexes composed of a metal, the amino acid of interest, and an auxiliary ligand.<sup>22</sup> This method was further explored by Siu et al. and O'Hair et

**Special Issue:** Peter B. Armentrout Festschrift

**Received:** May 16, 2012

**Revised:** August 24, 2012

**Published:** August 24, 2012



al.<sup>20,23,31</sup> Other chemical modifications followed by CID to generate radical species include peroxycarbamates attached to lysine<sup>27,30</sup> or to the N-terminus of a peptide,<sup>21</sup> serine nitrate esters,<sup>20,29</sup> and nitrosylated cysteine.<sup>28</sup> Another method to produce amino acid radical cations employs UV photodissociation of iodotyrosine<sup>25,26</sup> or modified phosphorylated serine and threonine.<sup>24</sup>

An emerging method for studying the structure of radical ions in the gas phase is infrared multiple photon dissociation (IRMPD) spectroscopy. For several years, IRMPD spectroscopy has been successfully used to determine the structure of protonated amino acids<sup>32–35</sup> and metal cationized amino acids and peptides,<sup>36–42</sup> including multiple contributions from the Armentrout group.<sup>37–39,41</sup> It has only been very recently that this technique has been used to study the structure of radical cations and anions. The first study by Steill et al. determined the structure of the histidine radical cation.<sup>43</sup> Since then, other structural studies on the cysteine radical cation,<sup>44</sup> the cysteine methyl ester radical cation,<sup>45</sup> the *N*-acetyl-cysteine radical cation and anion,<sup>46</sup> and the Gly-Cys and Cys-Gly dipeptides<sup>47</sup> have been performed. Theoretical calculations are also used in these studies and individually to determine structure.<sup>48</sup>

In the past, our group has employed a three-pronged approach to the study of cysteine radical ions, its derivatives, and peptides containing cysteine.<sup>45–47</sup> This approach involves IRMPD spectroscopy, DFT calculations, and ion–molecule reactions. Ion–molecule reactions can be used as a probe of radical structure<sup>20,29,49,50</sup> and can indicate the position of the radical in the structure.<sup>46,47</sup> Sulfur-based radicals, as has been shown by Kenttamaa et al., are reactive toward neutrals such as dimethyldisulfide and allyl iodide.<sup>51–56</sup> Meanwhile, carbon-based radicals are unreactive toward these neutrals, and instead react with dioxygen, NO, and NO<sub>2</sub>.<sup>20,57</sup> Our previous studies using these techniques have shown that in some cases radical migration from the sulfur atom to a more stable  $\alpha$ -carbon atom can occur.<sup>46,47</sup>

In this study, we continue our investigation of the cysteine radical cation and its derivatives by turning our attention to homocysteine (Hcy) radical cation. Homocysteine is an amino acid found in cells whose elevated levels are associated with several major pathologies.<sup>58</sup> Hcy differs from cysteine only by an extra methylene linkage in its side chain (Scheme 1). The

the difference in structures of Cys<sup>•+</sup> and Hcy<sup>•+</sup> is sufficient to allow the radical migration to occur in the gas phase.

## EXPERIMENTAL SECTION

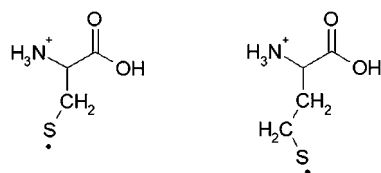
**Chemicals and Reagents.** All chemicals and reagents were used as received without any further purification. Cysteine, homocysteine, methanol (HPLC grade), *tert*-butylnitrite, and dimethyldisulfide were all purchased from Sigma-Aldrich (Milwaukee, WI).

**Ion–Molecule Reactions.** Ion–molecule reactions were carried out using a Bruker Esquire 3000 quadrupole ion trap mass spectrometer (Bruker Daltonics, Bremen, Germany) modified to conduct ion–molecule reactions as described previously.<sup>59</sup> Nitrosylated cysteine and homocysteine were generated by allowing a 1.5:1 mixture of *tert*-butylnitrite and a 1 mM solution of cysteine or homocysteine (in 50/50 methanol:water with 1% acetic acid) to react for 10 min at room temperature. The reaction mixture was diluted 100-fold using 50/50 methanol:water with 1% acetic acid and introduced into the ESI source of the mass spectrometer at a flow rate of 5  $\mu\text{L min}^{-1}$ . The sheath gas, capillary voltage, and temperature were adjusted to about 10 arbitrary units, 3.0 kV, and 250 °C, respectively. Radical cations of cysteine or homocysteine were produced by CID. When using CID, the protonated S-nitrosylated precursor was mass selected and then subjected to CID using a collision energy sufficient to dissociate the majority of the precursor ions. The radical ion was then mass selected and allowed to react with the neutral reagent introduced into the trap via a leak valve. The scan delay was varied from 0 to 5000 ms, allowing the acquisition of mass spectra at different reaction time points. The pressure of neutral dimethyldisulfide was about  $1 \times 10^{-8}$  Torr in the ion trap region, as estimated by fast ion–molecule reactions (the fastest reactions for dimethyldisulfide were the reaction with cysteine radical cation and with *N*-acetyl cysteine radical cation). By assuming the collision rate for these reactions, the pressure could be estimated. The polarizability (volume) of dimethyldisulfide needed for the collision rate calculation was estimated to be 15.8 Å<sup>3</sup> as described by Miller and Savchik.<sup>60</sup> The collision rate was calculated by using the Langevin equation.

### Infrared Multiple Photon Dissociation Spectroscopy.

IRMPD spectroscopy studies were carried out at the Free Electron Laser for Infrared eXperiments (FELIX) facility located at the FOM-Institute for Plasma Physics Rijnhuizen in Nieuwegein (The Netherlands).<sup>61</sup> The nitrosylated precursors were generated as described above with the slight modification that the end concentration was 1 mM. Once generated, the nitrosylated precursor was introduced into a custom-built FT-ICR mass spectrometer<sup>62</sup> equipped with an orthogonal Z-spray electrospray ionization source. Operating parameters for ESI were optimized to maximize formation and transfer of ions to the ICR cell. A dc potential switch was applied to the octopole ion guide to trap the ions in the ICR cell without using a gas pulse,<sup>63</sup> thus eliminating collisional heating of the ions. Protonated S-nitrosylated homocysteine was isolated using a stored waveform inverse Fourier transform (SWIFT) pulse, and subsequently irradiated for 0.25 s with a 40 W CO<sub>2</sub> laser in order to produce the radical cation via IRMPD. After a 5 s wait time, another SWIFT pulse isolates the homocysteine radical cation before being irradiated with the FELIX infrared laser. Spectra were collected by monitoring the efficiency of FELIX-induced IRMPD as a function of laser wavelength. To produce infrared spectra, the free electron laser

**Scheme 1. The Structures of the Cysteine Radical Cation and the Homocysteine Radical Cation**



sulfur-based radical of homocysteine is of interest because of its ability to migrate from the sulfur atom to the  $\alpha$ -carbon position much more easily (about 10 times faster in solution at pH 10) than in the cysteine radical.<sup>15</sup> The rate increase in this intramolecular rearrangement was explained by a less-hindered five-membered-ring transition state for homocysteine as compared to a strained four-membered ring transition state for cysteine.<sup>58</sup> S-to- $\alpha$ -carbon radical migration was not observed in Cys radical cation in the gas phase.<sup>46,47</sup> Here we investigate if

was scanned in 0.02–0.04  $\mu\text{m}$  increments between 5.5 and 10  $\mu\text{m}$  and the product ion and precursor ion intensities were measured at each step using the excite/detect sequence of the FT-ICR-MS<sup>64</sup> after irradiation with FELIX.<sup>65</sup> The IRMPD yield is determined by normalizing the fragment intensity to the total ion intensity, and linearly corrected for variations in FELIX power over the spectral range. Alternatively but less efficiently, the radical cation could be produced from the S-nitrosylated precursor by CID in the ion source. We verified that IR spectra of the radical cation produced by CID and by CO<sub>2</sub>-laser induced IRMPD are identical.

**Density Functional Theory Calculations.** All geometry optimizations and harmonic vibrational frequencies were calculated using the Gaussian 09 suite of programs<sup>66</sup> and the hybrid B3LYP functional. Initial geometry optimizations were performed using the relatively small 3-21G\* basis set. All minima located were reoptimized using the same functional and the 6-311++G(d,p) basis set. All transition state calculations were performed using the QST2 function within Gaussian. In most cases, intrinsic reaction coordinate (IRC) calculations were used to confirm that the transition states linked the correct minima that represent pre- and post-transformation structures. Vibrational frequency calculations were performed on the structures optimized at the B3LYP/6-311++G(d,p) level of theory and used to determine whether optimized structures were true minima (no imaginary frequencies) or transition states (one imaginary frequencies), for zero-point energy corrections to electronic energies (used unscaled), and for prediction of infrared spectra for comparison to experimental IRMPD spectra. For comparison of DFT spectra to IRMPD spectra, the computed frequencies were scaled by a factor of 0.98, which is known to be adequate at the current level of theory.<sup>67,68</sup> The intensities in the theoretical and experimental spectra were normalized (relative intensity).

## RESULTS AND DISCUSSION

Figure 1a and b show the mass spectra of the formation of the radical cation of cysteine (Figure 1a) and homocysteine (Figure 1b) from the CID of their nitrosylated precursors. Due to the way in which these ions are generated (homolytic cleavage of

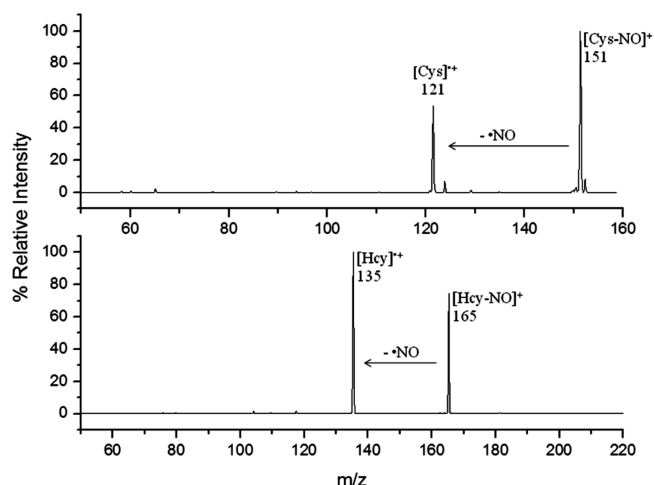
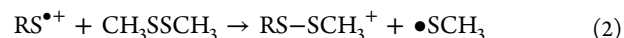


**Figure 1.** CID of (a) protonated nitrosylated cysteine ( $m/z$  151) to form the cysteine radical cation ( $m/z$  121) and (b) protonated nitrosylated homocysteine ( $m/z$  165) to form the homocysteine radical cation ( $m/z$  135).

the S–NO bond), the radical is initially formed on the sulfur atom (eq 1).



Figure 2 shows the kinetic plot for the reactivity of the cysteine radical cation and the homocysteine radical cation with dimethyldisulfide. It was observed that the reaction with dimethyl disulfide led to the addition of  $\bullet\text{SCH}_3$  (+47 Da) to both  $\text{Cys}^{\bullet+}$  ( $m/z$  121) and  $\text{Hcy}^{\bullet+}$  ( $m/z$  135), as shown in eq 2:



where  $\text{RS}^{\bullet+}$  is  $\text{Cys}^{\bullet+}$  or  $\text{Hcy}^{\bullet+}$  with the S-based radical position.

Several groups including ours have studied the reactivity of sulfur radicals toward dimethyl disulfide.<sup>45,46,50–55</sup> The products of these reactions are formed by the thiyl radical attacking a sulfur atom of dimethyl disulfide and cleaving the disulfide bond. This type of reaction is nearly thermoneutral; hence, it is not enthalpically driven. Instead, it is believed that a relatively low energy barrier for this attack allows for the forward progression of these reactions.

As can be seen in Figure 2, there is a difference in the kinetics of the reactions involving the cysteine and homocysteine radical cations. It is clear from the graph that the cysteine radical cation reacts more quickly with dimethyldisulfide than the homocysteine radical cation. In fact, the  $\text{Cys}^{\bullet+}$  reaction occurs at near-collision rate (one of the fastest we have observed with dimethyldisulfide neutral), while the  $\text{Hcy}^{\bullet+}$  reacts more than 2 times more slowly. The upper limit for the rate constant for the cysteine radical cation with dimethyldisulfide was calculated by the Langevin equation to be  $2 \times 10^{-9} \text{ cm}^3 \text{ molecule}^{-1} \text{ s}^{-1}$ . From this value, the upper limit for the rate constant for the homocysteine radical cation is  $8.6 \times 10^{-10} \text{ cm}^3 \text{ molecule}^{-1} \text{ s}^{-1}$ . Figure S1 (Supporting Information) shows the kinetic semilog plot of the reactivity of the radical cations of cysteine and homocysteine.

In order to investigate this difference in reactivity, IRMPD spectroscopy and DFT calculations were performed. Recent studies have shown that through the use of these techniques the structure and position of the radical in amino acid radical cations can be determined.<sup>43–47</sup> In previous studies, we have shown that for some cysteine-containing radical cations (where the radical is initially located on the sulfur) radical migration can occur through intermolecular hydrogen atom transfer (HAT) if the energy barrier is low enough.<sup>46,47</sup> This radical migration results in the radical being placed at an  $\alpha$ -carbon position, which is calculated to be lower in energy than the sulfur radical due to captodative resonance.<sup>69–71</sup> The  $\alpha$ -carbon radical has been shown to not be reactive toward dimethyl disulfide.<sup>29</sup> This would suggest that if radical migration occurs then the reactivity toward the neutral would stop, as has been shown previously for reactions with allyl iodide.<sup>47</sup>

On the basis of these observations, the IRMPD spectrum was obtained for the homocysteine radical cation and compared to calculated IR spectra to determine the structure and position of the radical (Figure 3). The  $\alpha$ -carbon radical was found to be 17.8 kJ/mol lower in energy than the sulfur radical. However, the comparison of the calculated IR spectra with the experimental IR spectrum shows that the sulfur radical displays a much better match (Figure 3a) than the  $\alpha$ -carbon radical (Figure 3b). The greatest difference between the two calculated IR spectra is in the carbonyl stretch of the  $-\text{COOH}$  moiety. For the sulfur radical, the carbonyl stretch occurs at about 1780  $\text{cm}^{-1}$  which shows a very good match to the experimental

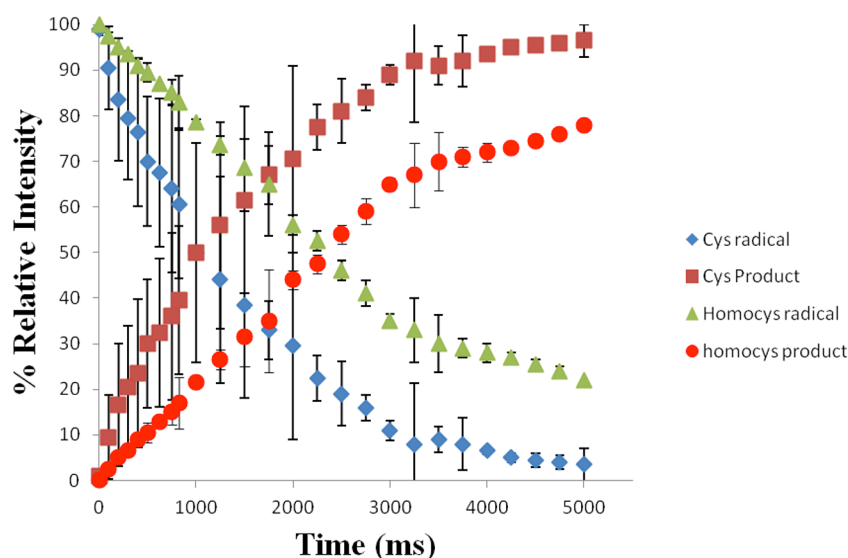


**Figure 2.** Kinetic plots of the reactions of dimethyldisulfide with the radical cations of cysteine and homocysteine generated by CID. The data are an average of three measurements. The kinetic semilog plots are given in Figure S1 (Supporting Information).

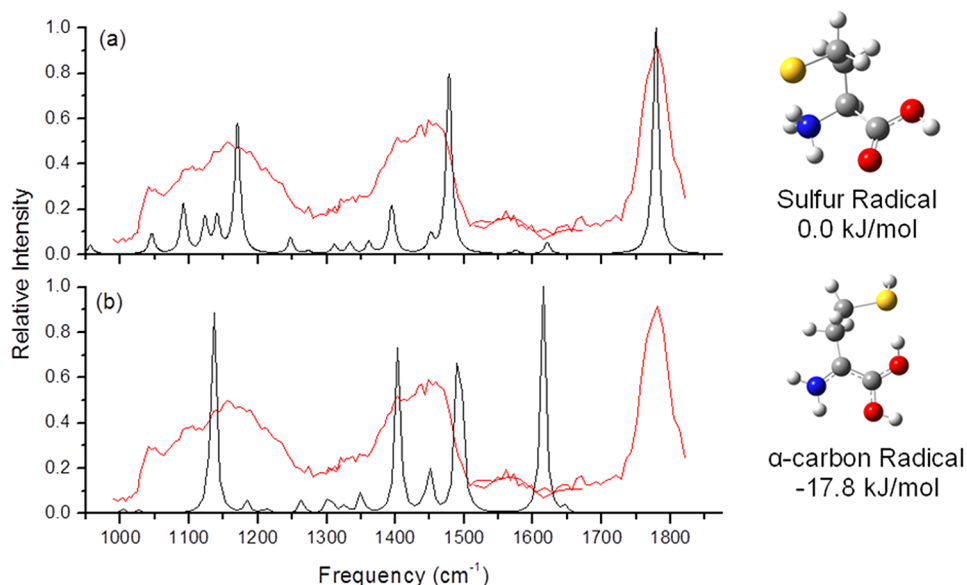


**Figure 3.** Comparison between experimental and theoretical IR spectra for homocysteine radical cation: (a) theoretical sulfur radical spectrum (0.0 kJ/mol) and (b) theoretical  $\alpha$ -carbon radical spectrum (−17.8 kJ/mol). The experimental spectrum (red trace) is overlaid on the theoretical spectra.

spectrum (shown in red). For the  $\alpha$ -carbon radical, the carbonyl stretch occurs at about  $1615\text{ cm}^{-1}$  and has no corresponding peak in the experimental IR spectrum. Sinha et al. obtained the gas-phase IR spectrum of the cysteine radical cation and found that for this system the radical is also retained on the sulfur atom.<sup>44</sup> Thus, both ion–molecule reactions and IRMPD spectroscopy suggest that the radical stays on the sulfur atom in  $\text{Hcy}^{\bullet+}$ .

Utilizing DFT calculations, we determined the lowest energy pathway through which the homocysteine radical cation would have to follow in order to rearrange to the  $\alpha$ -carbon species. Figure 4 shows the lowest energy pathway for rearrangement. This pathway (radical first, charge second) has a relatively high energy barrier of  $131.8\text{ kJ/mol}$  and involves an intramolecular hydrogen atom transfer from the  $\alpha$ -carbon atom to the sulfur atom followed by a proton transfer from the amine nitrogen to the carboxyl carbon. One other energetically demanding

pathway was calculated, with an even higher barrier (see Figure S2 in the Supporting Information). In this pathway, the migration of the radical and the proton are not simultaneous. In the highest energy pathway calculated (charge first, radical second, Figure S2 in the Supporting Information), the charge is transferred from the amine nitrogen to the carboxyl carbon (TS III,  $63.6\text{ kJ/mol}$ ) first and then the radical is transferred to the  $\alpha$ -carbon (TS IV,  $-13.1\text{ kJ/mol}$ ). The highest energy structure in this pathway is structure IV with an energy of  $160.2\text{ kJ/mol}$ , which has the charge located on the carboxyl group and the radical on the sulfur. This is a very unstable structure. It is of interest to compare the major barrier in the lowest energy structure for the rearrangement of  $\text{Hcy}^{\bullet+}$  (Figure 4) to that calculated for the S-to- $\alpha$ -carbon radical migration in  $\text{Cys}^{\bullet+}$ . Zhao et al. have calculated several rearrangement pathways for the cysteine radical cation, the lowest energy barrier being  $158.6\text{ kJ/mol}$ .<sup>48</sup> Our previous calculations<sup>45</sup> for  $\text{CysOMe}^{\bullet+}$



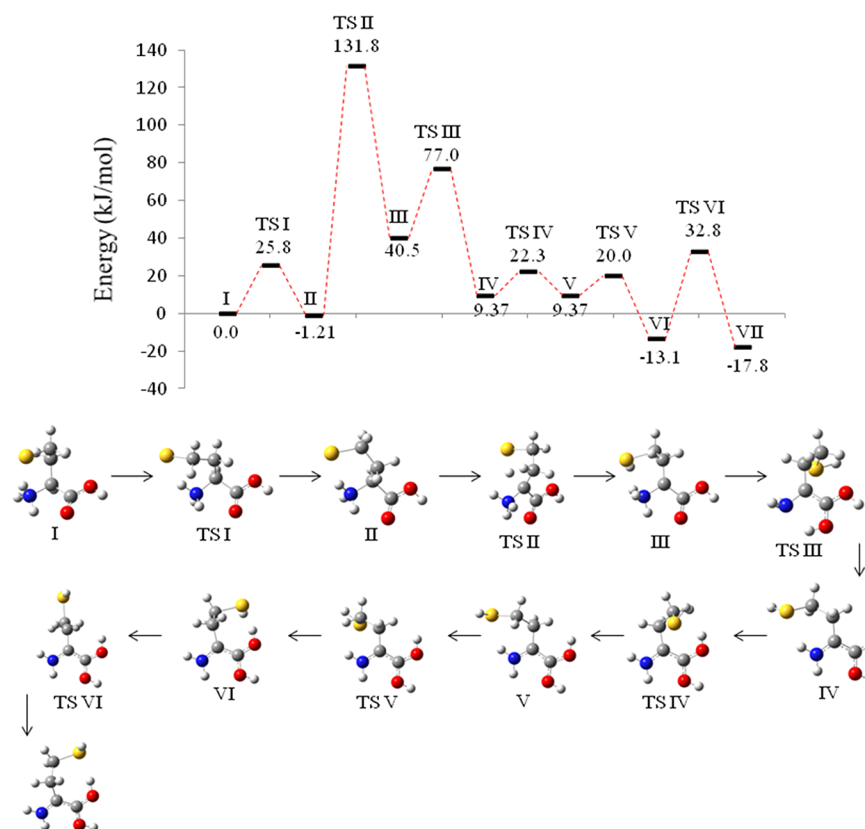


**Figure 4.** Calculated lowest energy pathway for the radical migration from the sulfur to the  $\alpha$ -carbon followed by charge transfer from the amine nitrogen to the carboxyl carbon for the radical cation of homocysteine.

showed similar barriers in the range 144–156 kJ/mol. Thus, while the extra methylene linkage in the Hcy radical cation lowers the rearrangement barrier to 131.8 kJ/mol, it is not enough to promote facile rearrangement under our experimental conditions. This correlates well with the recently studied Cys-Gly and Gly-Cys radical cations.<sup>47</sup> For Cys-Gly<sup>•+</sup>, the barrier was calculated to be 133.8 kJ/mol and the radical migration was not experimentally observed, while, for Gly-Cys<sup>•+</sup>, with an energy barrier of 62.8 kJ/mol, facile radical rearrangement was reported.<sup>47</sup>

The high energy barriers for both cysteine and homocysteine readily explain why no radical rearrangement is observed under our experimental conditions. This does not correlate with the solution phase, where homocysteine sulfur radical rearranges 10 times faster than the cysteine one.<sup>58</sup> There is, however, an important pH difference between our gas-phase results and the solution data. The reactions in solution were studied at pH 10 where Cys and Hcy radicals are *deprotonated* at the C terminus (i.e., they are radical anions). In our gas-phase study, Cys and Hcy sulfur radicals are *protonated* at the N terminus, leading to radical cations. Having the N terminus protonated does not promote the ready formation of the captodative,  $\alpha$ -carbon-based radical. Instead formation of such a stabilized radical requires an extra step involving intramolecular proton transfer from the amino group to the carbonyl, thus increasing the overall barrier for rearrangement. This explanation is in good agreement with findings of Schoneich, who showed that if the charge is located on the amine nitrogen, the rearrangement rate decreases about 10-fold.<sup>19</sup> Studies are underway in our laboratory to further explore this hypothesis by studying the homocysteine radical anion.

The results described above highlight that radical migration from the sulfur atom is not responsible for the difference in reactivity between Hcy<sup>•+</sup> and Cys<sup>•+</sup>. A comparison of the two lowest energy structures of the cysteine and homocysteine radical cations with the radical located on the sulfur in both cases (figure 5) suggests that intramolecular hydrogen bonding

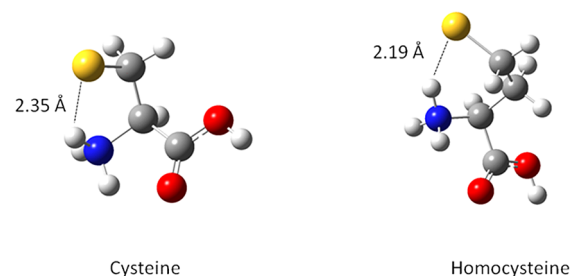


**Figure 5.** Low-energy structures of radical cations of (a) cysteine and (b) homocysteine. Structures show the length for the hydrogen bond between the sulfur radical and a hydrogen covalently bound to the amine nitrogen.

between the sulfur radical and a hydrogen of the N-terminal amino group may be responsible for modulation of the reactivity of the radical site. The hydrogen bond length in cysteine is 2.35 Å, while the hydrogen bond length in homocysteine is 2.19 Å. The hydrogen bond in homocysteine is shorter perhaps because of the lack of steric constraints due to the extra carbon located in the side chain as compared to cysteine. Since the sulfur radical of the homocysteine radical cation has a stronger hydrogen bond with the amine hydrogen

than the cysteine radical cation, it is possible that this is why it is less reactive than the cysteine radical cation.

Hydrogen bonding is known to affect the reactivity of gas-phase ions.<sup>72–75</sup> For example, Chen et al. found that hydrogen bonding can lower the intrinsic nucleophilicity of solvated nucleophiles.<sup>72</sup> Reports of similar effects on the structure and reactivity of radicals have been scarce. Recent work by Mitroka et al. showed that the reactivity of hydroxyl radical both in solution and in the gas phase can be modulated by hydrogen bonding to water molecules.<sup>76</sup> Another example is the stabilization of phenoxyl radicals by both intramolecular and intermolecular hydrogen bonding.<sup>77–79</sup> Our study gives a different example where intramolecular hydrogen bonding stabilization of thiyl aliphatic radicals may potentially affect their reactivity.

## CONCLUSIONS

The radical cation of homocysteine can easily be formed through the dissociation of the protonated S-nitrosylated precursor. By virtue of cleaving the S–NO bond, the radical is initially located on the sulfur atom. No rearrangement to the more stable,  $\alpha$ -carbon-based radical species was observed via ion–molecule reactions or IRMPD spectroscopy. This was explained by a relatively high barrier (131.8 kJ/mol), consistent with cysteine and cysteine methyl ester radical cation cases where no radical migration was observed either.

Comparison of the reactivity of  $\text{Hcy}^{\bullet+}$  versus  $\text{Cys}^{\bullet+}$  in ion–molecule reactions with dimethyl disulfide showed that the cysteine radical cation reacts ca. 2.3 times more quickly than the homocysteine radical cation. We suggest that the degree of hydrogen bonding between the sulfur atom and a hydrogen of the protonated N terminus (2.35 Å for  $\text{Cys}^{\bullet+}$  and 2.19 Å for  $\text{Hcy}^{\bullet+}$ ) may be one of the factors that explain this difference in reactivity. Work is underway to use high level electronic structure calculations to define the role of intramolecular hydrogen bonding in the reactions of radicals.

## ASSOCIATED CONTENT

### Supporting Information

Figures showing the kinetic data shown in Figure 2 displayed in semilog format and the calculated higher-energy pathway for radical rearrangement in homocysteine radical cation. This material is available free of charge via the Internet at <http://pubs.acs.org>.

## AUTHOR INFORMATION

### Corresponding Author

\*E-mail: [ryzhov@niu.edu](mailto:ryzhov@niu.edu).

### Notes

The authors declare no competing financial interest.

## ACKNOWLEDGMENTS

S.O., T.B., and V.R. acknowledge support from Northern Illinois University, and S.O. would also like to acknowledge support from a travel grant from the Center for Biochemical and Biophysical Studies of NIU. R.A.J.O. thanks the ARC Centre of Excellence in Free Radical Chemistry and Biotechnology for financial support. J.O. and G.B. are supported by the Nederlandse Organisatie voor Wetenschappelijk Onderzoek (NWO). We gratefully acknowledge the skillful assistance of the FELIX staff. This work is dedicated to

Prof. Peter B. Armentrout whose contributions to gas-phase ion chemistry will inspire generations of scientists.

## REFERENCES

- (1) Balagopalakrishna, C.; Abugo, O.; Horsky, J.; Manoharan, P.; Nagababu, E.; Rifkind, J. *Biochemistry* **1998**, *37*, 13194–13202.
- (2) Becker, A.; Kabsch, W. *J. Biol. Chem.* **2002**, *277*, 40036–40042.
- (3) Ehrenberg, A.; Reichard, P. *J. Biol. Chem.* **1972**, *247*, 3485–3488.
- (4) Hioe, J.; Savasci, G.; Brand, H.; Zipse, H. *Chem.—Eur. J.* **2011**, *17*, 3781–3789.
- (5) Knauer, S. H.; Buckel, W.; Dobbek, H. *J. Am. Chem. Soc.* **2011**, *133*, 4342–4347.
- (6) Lepore, B.; Ruzicka, F.; Frey, P.; Ringe, D. *Proc. Natl. Acad. Sci. U.S.A.* **2005**, *102*, 13819–13824.
- (7) Licht, S.; Gerfen, G.; Stubbe, J. *Science* **1996**, *271*, 477–481.
- (8) Logan, D.; Andersson, J.; Sjöberg, B.-M.; Nordlund, P. *Science* **1999**, *283*, 1499–1504.
- (9) Mozziconacci, O.; Sharov, V.; Williams, T.; Kerwin, B.; Schoneich, C. *J. Phys. Chem. B* **2008**, *112*, 9250–9257.
- (10) Nausner, T.; Casi, G.; Koppenol, W.; Schoneich, C. *J. Phys. Chem. B* **2008**, *112*, 15034–15044.
- (11) Reitzer, R.; Gruber, K.; Jögl, G.; Wagner, U.; Bothe, H.; Buckel, W.; Kratky, C. *Structure* **1999**, *7*, 891–902.
- (12) Sivaraja, M.; Goodin, D.; Smith, M.; Hoffman, B. *Science* **1989**, *245*, 738–740.
- (13) Davies, M. *Arch. Biochem. Biophys.* **1996**, *336*, 163–172.
- (14) Davies, M. *J. Clin. Biochem. Nutr.* **2011**, *48*, 8–19.
- (15) *Radical-mediated Protein Oxidation*; Davies, M., Dean, R., Eds.; Oxford University Press: New York, 1997.
- (16) Headlam, H.; Mortimer, A.; Easton, C.; Davies, M. *Chem. Res. Toxicol.* **2000**, *13*, 1087–1095.
- (17) Rauk, A.; Armstrong, D. *J. Am. Chem. Soc.* **2000**, *122*, 4185–4192.
- (18) Rauk, A.; Yu, D.; Armstrong, D. *J. Am. Chem. Soc.* **1998**, *120*, 8848–8855.
- (19) Schoneich, C. *Chem. Res. Toxicol.* **2008**, *21*, 1175–1179.
- (20) Barlow, C. K.; Wright, A.; Easton, C. J.; O'Hair, R. A. J. *Org. Biomol. Chem.* **2011**, *9*, 3733–3745.
- (21) Chacon, A.; Masterson, D. S.; Yin, H.; Liebler, D. C.; Porter, N. A. *Bioorg. Med. Chem.* **2006**, *14*, 6213–6222.
- (22) Chu, I. K.; Rodriguez, C. F.; Lau, T.-C.; Hopkinson, A. C.; Siu, K. W. M. *J. Phys. Chem. B* **2000**, *104*, 3393–3397.
- (23) Chu, I. K.; Zhao, J.; Xu, M.; Siu, S. O.; Hopkinson, A. C.; Siu, K. W. M. *J. Am. Chem. Soc.* **2008**, *130*, 7862–7872.
- (24) Diedrich, J.; Julian, R. *J. Am. Chem. Soc.* **2008**, *130*, 12212–12213.
- (25) Liu, Z.; Julian, R. *J. Am. Soc. Mass Spectrom.* **2009**, *20*, 965–971.
- (26) Ly, T.; Julian, R. *J. Am. Chem. Soc.* **2008**, *130*, 351–358.
- (27) Masterson, D. S.; Yin, H.; Chacon, A.; Hachey, D. L.; Norris, J. L.; Porter, N. A. *J. Am. Chem. Soc.* **2004**, *126*, 720–721.
- (28) Ryzhov, V.; Lam, A.; O'Hair, R. A. J. *J. Am. Soc. Mass Spectrom.* **2009**, *20*, 985–995.
- (29) Wee, S.; Mortimer, A.; Moran, D.; Wright, A.; Barlow, C. K.; O'Hair, R. A. J.; Radom, L.; Easton, C. J. *Chem. Commun.* **2006**, 4233–4235.
- (30) Yin, H.; Chacon, A.; Porter, N.; Masterson, D. *J. Am. Soc. Mass Spectrom.* **2007**, *18*, 807–816.
- (31) Barlow, C. K.; McFadyen, W. D.; O'Hair, R. A. J. *J. Am. Chem. Soc.* **2005**, *127*, 6109–6115.
- (32) Coletti, C.; Re, N.; Scuderi, D.; Maitre, P.; Chiavarino, B.; Fornarini, S.; Lanucara, F.; Sinha, R. K.; Crestoni, M. E. *Phys. Chem. Chem. Phys.* **2010**, *12*, 13455–13467.
- (33) Dunbar, R. C.; Steill, J. D.; Polfer, N. C. *Int. J. Mass Spectrom.* **2009**, *283*, 77–84.
- (34) Mino, W. K., Jr.; Gulyuz, K.; Wang, D.; Stedwell, C. N.; Polfer, N. C. *J. Phys. Chem. Lett.* **2011**, *2*, 299–304.
- (35) Steill, J. D.; Szczepanski, J.; Oomens, J.; Eyler, J. R.; Brajter-Toth, A. *Anal. Bioanal. Chem.* **2011**, *399*, 2463–2473.

- (36) Bush, M. F.; Oomens, J.; Saykally, R. J.; Williams, E. R. *J. Am. Chem. Soc.* **2008**, *130*, 6463–6471.
- (37) Citir, M.; Hinton, C. S.; Oomens, J.; Steill, J. D.; Armentrout, P. B. *J. Phys. Chem. A* **2012**, *116*, 1532–1541.
- (38) Citir, M.; Stennett, E. M. S.; Oomens, J.; Steill, J. D.; Rodgers, M. J.; Armentrout, P. B. *Int. J. Mass Spectrom.* **2010**, *297*, 9–17.
- (39) Dray, M. K.; Armentrout, P. B.; Oomens, J.; Schäfer, M. *Int. J. Mass Spectrom.* **2010**, *297*, 18–27.
- (40) Dunbar, R. C.; Steill, J. D.; Oomens, J. *Phys. Chem. Chem. Phys.* **2010**, *12*, 13383–13393.
- (41) Hofstetter, T. E.; Howder, C.; Berden, G.; Oomens, J.; Armentrout, P. B. *J. Phys. Chem. B* **2011**, *115*, 12648–12661.
- (42) O'Brien, J. T.; Prell, J. S.; Berden, G.; Oomens, J.; Williams, E. R. *Int. J. Mass Spectrom.* **2010**, *297*, 116–123.
- (43) Steill, J.; Zhao, J.; Siu, C.-K.; Ke, Y.; Verkerk, U.; Oomens, J.; Dunbar, R. C.; Hopkinson, A. C.; Siu, K. W. M. *Angew. Chem.* **2008**, *120*, 154–156.
- (44) Sinha, R.; Maitre, P.; Piccirillo, S.; Chiavarino, B.; Crestoni, M.; Fornarini, S. *Phys. Chem. Chem. Phys.* **2010**, *12*, 9794–9800.
- (45) Osburn, S.; Steill, J.; Oomens, J.; O'Hair, R. A. J.; Van Stipdonk, M.; Ryzhov, V. *Chem.—Eur. J.* **2010**, *17*, 873–879.
- (46) Osburn, S.; Berden, G.; Oomens, J.; O'Hair, R. A. J.; Ryzhov, V. *J. Am. Soc. Mass Spectrom.* **2011**, *22*, 1794–1803.
- (47) Osburn, S.; Berden, G.; Oomens, J.; O'Hair, R. A. J.; Ryzhov, V. *J. Am. Soc. Mass Spectrom.* **2012**, *23*, 1019–1023.
- (48) Zhao, J.; Siu, K. W. M.; Hopkinson, A. C. *Phys. Chem. Chem. Phys.* **2008**, *10*, 281–288.
- (49) Fu, M.; Li, S.; Archibold, E.; Yurkovich, M.; Nash, J.; Kenttamaa, H. J. *Am. Soc. Mass Spectrom.* **2010**, *21*, 1737–1752.
- (50) Li, S.; Fu, M.; Habicht, S.; Nash, J. J.; Kenttamaa, H. I. *J. Org. Chem.* **2009**, *74*, 7724–7732.
- (51) Adeuya, A.; Price, J. M.; Jankiewicz, B. J.; Nash, J. J.; Kenttamaa, H. I. *J. Phys. Chem. A* **2009**, *113*, 13663–13674.
- (52) Heidbrink, J. L.; Ramirez-Arizmendi, L. E.; Thoen, K. K.; Guler, L.; Kenttamaa, H. I. *J. Phys. Chem. A* **2001**, *105*, 7875–7884.
- (53) Jankiewicz, B. J.; Reece, J. N.; Vinuesa, N. R.; Nash, J. J.; Kenttamaa, H. I. *Angew. Chem., Int. Ed.* **2008**, *47*, 9860–9865.
- (54) Kenttamaa, H. I. *Org. Mass Spectrom.* **1994**, *29*, 1–10.
- (55) Stirk, K. M.; Kiminkinen, L. K. M.; Kenttamaa, H. I. *Chem. Rev.* **1992**, *92*, 1649–1665.
- (56) Tichey, S.; Thoen, K.; Price, J.; Ferra, J.; Petucci, C.; Kenttamaa, H. I. *J. Org. Chem.* **2001**, *66*, 2726–2733.
- (57) Kirk, B. B.; Harman, D. G.; Blanksby, S. J. *J. Phys. Chem. A* **2010**, *114*, 1446–1456.
- (58) Sibrian-Vazquez, M.; Escobedo, J.; Lim, S.; Samoei, G.; Strongin, R. *Proc. Natl. Acad. Sci. U.S.A.* **2010**, *107*, 551–554.
- (59) Pyatkivskyy, Y.; Ryzhov, V. *Rapid Commun. Mass Spectrom.* **2008**, *22*, 1288–1294.
- (60) Miller, K. J.; Savchik, J. A. *J. Am. Chem. Soc.* **1979**, *101*, 7206–7213.
- (61) Oepts, D.; Van Der Meer, A.; Van Amersfoort, P. *Infrared Phys. Technol.* **1995**, *36*, 297–308.
- (62) Valle, J.; Eyler, J.; Oomens, J.; Moore, D.; Van Der Meer, A.; Von Helden, G.; Meijer, G.; Hendrickson, C.; Marshall, A.; Blakney, G. *Rev. Sci. Instrum.* **2005**, *76*, 023103.
- (63) Polfer, N. C.; Oomens, J.; Moore, D.; Von Helden, G.; Meijer, G.; Dunbar, R. C. *J. Am. Chem. Soc.* **2006**, *128*, 517–526.
- (64) Marshall, A.; Hendrickson, C.; Jackson, G. *Mass Spectrom. Rev.* **1998**, *17*, 1–35.
- (65) Polfer, N. C.; Oomens, J. *Phys. Chem. Chem. Phys.* **2007**, *9*, 3804–3817.
- (66) Frisch, M. J.; Trucks, G. W.; Schlegel, H. B.; Scuseria, G. E.; Robb, M. A.; Cheeseman, J. R.; Montgomery, J. A., Jr.; Vreven, T.; Kudin, K. N.; Burant, J. C.; et al. *Gaussian 09*, revision D.01; Gaussian Inc.: Wallingford, CT, 2009.
- (67) Polfer, N. C.; Oomens, J.; Dunbar, R. C. *Phys. Chem. Chem. Phys.* **2006**, *8*, 2744–2751.
- (68) Polfer, N. C.; Oomens, J.; Dunbar, R. C. *ChemPhysChem* **2008**, *9*, 579–589.
- (69) Bordwell, F. G.; Zhang, X.; Alnajjar, M. S. *J. Am. Chem. Soc.* **1992**, *114*, 7623–7629.
- (70) Easton, C. J. *Chem. Rev.* **1997**, *97*, 53–82.
- (71) Sustmann, R.; Korth, H. G. *Adv. Phys. Org. Chem.* **1990**, *26*, 131–178.
- (72) Chen, X.; Brauman, J. I. *J. Am. Chem. Soc.* **2008**, *130*, 15038–15046.
- (73) Cheng, X.; Wu, Z.; Fenselau, C. J. *Am. Chem. Soc.* **1993**, *115*, 4844–4848.
- (74) Farrugia, J. M.; O'Hair, R. A. J. *Int. J. Mass Spectrom.* **2003**, *222*, 229–242.
- (75) Sharma, R. B.; Kebarle, P. J. *Am. Chem. Soc.* **1984**, *106*, 3913–3916.
- (76) Mitroka, S.; Zimmeck, S.; Troya, D.; Tanko, J. M. *J. Am. Chem. Soc.* **2010**, *132*, 2907–2913.
- (77) Amorati, R.; Pedulli, G. F.; Geuerra, M. *Org. Biomol. Chem.* **2010**, *8*, 3136–3141.
- (78) Amorati, R.; Valgimigli, L. *Org. Biomol. Chem.* **2012**, *10*, 4147–4158.
- (79) Pratt, D. A.; DiLabio, G. A.; Valgimigli, L.; Pedulli, G. F.; Ingold, K. U. *J. Am. Chem. Soc.* **2002**, *124*, 11085–11092.